

KCNQ5, a Novel Potassium Channel Broadly Expressed in Brain, Mediates M-type Currents*

Received for publication, April 17, 2000, and in revised form, May 16, 2000
Published, JBC Papers in Press, May 17, 2000, DOI 10.1074/jbc.M003245200

Björn C. Schroeder, Mirko Hechenberger, Frank Weinreich, Christian Kubisch‡, and Thomas J. Jentsch§

From the Zentrum für Molekulare Neurobiologie Hamburg, Hamburg University, Martinistrasse 85, D-20246 Hamburg, Germany

KCNQ2 and KCNQ3, both of which are mutated in a type of human neonatal epilepsy, form heteromeric potassium channels that are expressed in broad regions of the brain. The associated current may be identical to the M-current, an important regulator of neuronal excitability. We now show that the RNA encoding the novel KCNQ5 channel is also expressed in brain and in sympathetic ganglia where it overlaps largely with KCNQ2 and KCNQ3. In addition, it is expressed in skeletal muscle. KCNQ5 yields currents that activate slowly with depolarization and can form heteromeric channels with KCNQ3. Currents expressed from KCNQ5 have voltage dependences and inhibitor sensitivities in common with M-currents. They are also inhibited by M1 muscarinic receptor activation. A KCNQ5 splice variant found in skeletal muscle displays altered gating kinetics. This indicates a molecular diversity of channels yielding M-type currents and suggests a role for KCNQ5 in the regulation of neuronal excitability.

Mutations in all four known *KCNQ* potassium channel genes cause human inherited disease. Mutations in *KCNQ1* (also known as *KvLQT1*) lead to cardiac arrhythmias in the long QT syndrome (1) that are associated with congenital deafness in the recessive Jervell and Lange-Nielsen syndrome (2). Mutations in either *KCNQ2* or *KCNQ3* lead to benign familial neonatal convulsions (BFNC),¹ a neonatal generalized epilepsy (3–5). Finally, mutations in *KCNQ4* cause autosomal dominant progressive hearing loss (6).

The expression of *KCNQ2* and *KCNQ3* appears to be restricted to the nervous system (3, 7). Both subunits are co-expressed in many areas of the brain, including the cortex, hippocampus, and thalamus (7, 8), suggesting the formation of heteromeric *KCNQ2/3* channels. This was supported by functional expression in *Xenopus* oocytes. Currents obtained by co-expressing both subunits were more than 10-fold larger than those obtained from homomeric channels (7, 9, 10), and domi-

nant negative mutations in either subunit suppressed currents from heteromeric channels (7). Currents of *KCNQ2/3* heteromers resemble M-currents (11) in their voltage dependence, kinetics, and sensitivity to inhibitors such as linopirdine and XE991 (10, 12). M-currents are defined by their electrophysiological and pharmacological characteristics. These potassium currents are already present at the slightly depolarized potentials at the threshold of action potential firing and are highly regulated by several second messenger pathways (13). M-currents are inhibited by the activation of muscarinic receptors (11, 13–15). Since regulation of M-currents provides a means to set the firing rate of neurons, it is plausible that a loss of M-current leads to neuronal hyperexcitability and epilepsy in BFNC. Moderate changes in the magnitude of these currents may have profound effects. It was estimated from heterologous expression of channel mutants found in BFNC that a 25% loss of *KCNQ2/KCNQ3* current may suffice to cause epilepsy (7).

As “M-currents” are defined by a rather broad set of biophysical and pharmacological characteristics, *KCNQ2* and *KCNQ3* subunits may not be the only molecular basis for these currents. Indeed, *eag*-related channels share some features with M-type currents, but opinions differ as to whether they really qualify as M-currents (16–19). Furthermore, the voltage and time dependence of *KCNQ4* is similar to that of *KCNQ2/3* channels, and *KCNQ4* is also inhibited by blockers of M-currents such as linopirdine, albeit with lower efficiency (6). The sensitivity to these inhibitors was increased in *KCNQ3/4* heteromers, suggesting that channels containing *KCNQ4* may underlie some forms of M-currents (6). Furthermore, *KCNQ4* is also inhibited by muscarinic stimulation (20). In contrast to *KCNQ2* and *KCNQ3*, however, *KCNQ4* plays an important role in hearing (6), and its expression in the central nervous system is restricted to some areas of the brainstem. This includes nuclei and tracts of the auditory pathway (21).

MATERIALS AND METHODS

Cloning and Functional Expression of KCNQ5—A partial cDNA encoding a novel *KCNQ* channel fragment was isolated by screening a human thalamus cDNA library (CLONTECH) using a *KCNQ3* cDNA as a probe. It was extended by 5'- and 3'-rapid amplification of cDNA ends techniques using a Marathon kit (CLONTECH) of human adult brain cDNA. The *KCNQ5* gene was localized on human chromosome spreads using fluorescent *in situ* hybridization by Genome Systems. The *KCNQ5* cDNA (all splice variants of Fig. 1B) was cloned into pTPN, a derivative of the *Xenopus* oocyte expression vector pTLN (22) which contains an additional *PacI* site 3' to the *NruI* site. After linearization with *HpaI*, capped cRNA was transcribed using SP6 RNA polymerase in the mMessage mMachine kit (Ambion). *Xenopus* oocytes were prepared by collagenase treatment, injected with 10 ng of cRNA, and incubated for 2–3 days at 17 °C. A dominant negative *KCNQ5* mutant (G278S) and a *KCNQ3* mutant (T323Y) were constructed by recombinant PCR. In some experiments, *KCNQ5* (or the G278S mutant) was co-expressed at a 1:1 ratio with *KCNQ2* or *KCNQ3*, or the respective

* This work was supported by grants from the Deutsche Forschungsgemeinschaft and the Fonds der Chemischen Industrie. The costs of publication of this article were defrayed in part by the payment of page charges. This article must therefore be hereby marked “advertisement” in accordance with 18 U.S.C. Section 1734 solely to indicate this fact.

The nucleotide sequence(s) reported in this paper has been submitted to the GenBank™/EBI Data Bank with accession number(s) AF202977.

‡ Present address: Institut für Humangenetik, Universität Bonn, Wilhelmstrasse 31, D-53111 Bonn, Germany.

§ To whom correspondence should be addressed. Tel.: 49-40-42803-4741; Fax: 49-40-42803-4839; E-mail: Jentsch@plexus.uke.uni-hamburg.de.

¹ The abbreviations used are: BFNC, benign familial neonatal convulsions; TEA, tetraethylammonium; WT, wild type; PCR, polymerase chain reaction.

dominant negative mutants KCNQ2(G279S) and KCNQ3(G318S) (7), or the KCNQ3(T323Y) mutant using again a total cRNA amount of 10 ng per oocyte. The human M1 receptor cDNA was obtained by PCR amplification from human fetal brain cDNA (CLONTECH) and was cloned into the pTPN vector. 10 and 5 ng of KCNQ5 and M1 receptor cDNAs, respectively, were co-injected into *Xenopus* oocytes. Conventional two-electrode voltage clamp measurements were performed at room temperature in ND96 saline (96 mM NaCl, 2 mM KCl, 1.8 mM CaCl₂, 1 mM MgCl₂, 5 mM HEPES, pH 7.4) using a Turbotec (npi Instruments) amplifier and pClamp (Axon Instruments) software. For cation selectivity measurements, NaCl was replaced by equimolar amounts of the respective chloride salt. When using TEA-chloride, this inhibitor replaced equivalent amounts of NaCl. For experiments examining the effect of muscarinic receptor stimulation, 1.6 mM Ca²⁺ was replaced by Mg²⁺ to reduce the activation of endogenous Ca²⁺-activated chloride channels.

Tail current analysis was used to estimate apparent P_{open} (Fig. 4). From a holding potential of -80 mV, oocytes were clamped to values between -100 and $+40$ mV for 2 s. Since variant III does not reach steady-state activation even after more than 10 s, the parameters obtained for this splice form do not reflect steady-state values. Tail currents were measured at -30 mV by extrapolating to the time when the voltage was changed. Since channel gating is slow compared with the voltage jump, these currents are proportional to the number of channels that are open at the prepulse voltage.

Northern Blot and in Situ Hybridization—Multiple tissue Northern blots (CLONTECH human 7760-1, human brain II 7755-1, and human brain III 7750-1) were hybridized overnight at 68 °C in 7% SDS, 10% polyethylene glycol 6000, 1.5× SSPE (SSPE, 150 mM NaCl, 10 mM NaH₂PO₄, 1 mM EDTA, pH 7.4), 100 μg/ml denatured herring sperm DNA with a ³²P-labeled *AflIII/EcoRI* fragment of pTPN-KCNQ5 that covers the last 1.1 kilobase pairs of the open reading frame. Blots were washed three times for 40 min in 0.1% SDS in 0.1× SSC (SSC, 150 mM NaCl, 15 mM sodium citrate, pH 7.0) at 50 °C and exposed on X-Omat film (Eastman Kodak Co.). mRNA was isolated from the NG108-15 cell line using the Trizol reagent (Life Technologies, Inc.) and oligo(dT) Dynabeads (Dynal), and 1.8 μg per lane were separated on a gel containing formaldehyde. The RNA was transferred to Hybond-N membrane and probed with a human KCNQ3 and a rat KCNQ5 probe. For the *in situ* hybridization of rat brain sections, a 1.1-kilobase pair rat KCNQ5 fragment (obtained by PCR and covering the equivalent region of 170–1290 base pairs of human KCNQ5) was subcloned into pBlue-script, and radioactive sense and antisense cRNAs were transcribed (Maxiscript, Ambion) using T3 and T7 RNA polymerase, respectively, and hydrolyzed to roughly 200–300-base pair fragments. *In situ* hybridization was performed as described (23). The rat brain sections were exposed to film, and the rat superior cervical ganglion section was dipped in a photoemulsion.

RESULTS

Primary Structure and Tissue Distribution of KCNQ5—By homology screening of a human brain cDNA library with KCNQ3, we isolated a novel member of the *KCNQ* gene family that we named *KCNQ5* (Fig. 1). It encodes a protein of 897 amino acids that has a predicted molecular mass of ~99 kDa. It has six transmembrane domains, a P-loop, and a carboxyl-terminal conserved cytoplasmic region (the “A-domain”) (24) (which may be involved in subunit interactions (25)) like the other four known *KCNQ* proteins with which it shares roughly 40% overall identity. Similar to other *KCNQ* channel cDNAs (3, 8, 26), we detected several splice variants in the cytoplasmic, carboxyl-terminal tail (Fig. 1B). Most of our functional studies were performed with variant I, which we had isolated from brain.

By using fluorescent *in situ* hybridization of human metaphase cells, the *KCNQ5* gene was localized to the long arm of chromosome 6 (6q14). Northern analysis revealed that *KCNQ5* is mainly expressed in brain and skeletal muscle (Fig. 2A). Its mRNA is present in many regions of the human brain, including the cerebral cortex, occipital pole, frontal and temporal lobes, putamen, and the hippocampus (Fig. 2B). In these regions, it is co-expressed with KCNQ2 (3) and KCNQ3 (7). Some regions that express significant levels of KCNQ2 or KCNQ3 (e.g. cerebellum, medulla, and thalamus) (7, 8) express only low

to undetectable levels of KCNQ5. *In situ* hybridization of rat brain sections largely confirmed this distribution of KCNQ5 within the central nervous system (Fig. 3A). In addition, it revealed significant expression in the piriform cortex, the entorhinal cortex, the pontine medulla, and the facial nucleus. In apparent contrast to the human Northern analysis (Fig. 2B), there was also a faint signal in the rat cerebellum (Fig. 3A). A weak expression in the rat cerebellum was subsequently confirmed by Northern analysis (data not shown).

M-currents have often been studied in sympathetic neurons (10–12, 14, 15, 27–29). This includes neurons of the rat superior cervical ganglion, which has recently been shown (10) to express both KCNQ2 and KCNQ3. *In situ* hybridization revealed that this ganglion also expresses KCNQ5 (Fig. 3C). A system frequently used to study neuronal M-currents is the NG108-15 mouse neuroblastoma × rat glioma cell line. These cells were recently shown to co-express KCNQ2 and KCNQ3 (18, 19). Northern analysis revealed that these cells also express KCNQ5 (Fig. 2C). Thus, this cell type expresses all three subunits.

Properties of KCNQ5 Channels—We expressed the three splice variants of KCNQ5 (Fig. 1B) in *Xenopus* oocytes and investigated the associated currents by two-electrode voltage clamping. Since there were no conspicuous differences between variants I and II, we focused on variants I and III that we had isolated from brain and skeletal muscle, respectively. Both forms of KCNQ5 yielded currents that needed several seconds to activate fully upon depolarization (Fig. 4, A and B). This activation was faster than with KCNQ4 (6) but slower than with KCNQ2 (3) (see also Fig. 7B) and in particular KCNQ1 (30, 31). Interestingly, gating kinetics differed markedly between both splice forms. The muscle isoform III showed a faster initial activation but did not reach steady-state activation even after 10 s. By contrast, the brain isoform I initially activated more slowly but reached steady-state after 2–3 s (for time constants, see legend to Fig. 4). This difference in gating kinetics is also apparent when a typical M-current voltage clamp protocol is employed. Although the brain variant yields currents that kinetically resemble M-currents (Fig. 4C), the muscle variant III does not show the typical current relaxations after hyperpolarizing voltage steps (Fig. 4D).

Tail current analysis was used to estimate activation parameters. Both variants begin to activate at voltages around -60 mV and show a decrease in apparent P_{open} at voltages more positive than approximately $+20$ mV (Fig. 4, E and F). This may be due to an inactivation process at positive voltages as observed, e.g. with KCNQ1 (32, 33). The apparent half-maximal activation did not show a large difference between these isoforms ($V_{1/2} \sim -46 \pm 1$ mV and $V_{1/2} \sim -48 \pm 1$ mV for isoforms I and III, respectively). This is more negative than with KCNQ4 ($V_{1/2} \sim -10$ mV) (6), but it is in the same range as values for KCNQ2 ($V_{1/2} \sim -37$ mV) (3) and KCNQ2/3 heteromers ($V_{1/2} \sim -40$ mV) (10). It fits nicely with values measured for native M-currents in cervical sympathetic ganglion cells ($V_{1/2} \sim -45$ mV) (10). Ion substitution experiments (Fig. 4G) revealed that KCNQ5 currents (isoform I) are highly selective for potassium. Other experiments (not shown) yielded a $Rb^+ \sim K^+ > Cs^+ > Na^+$ selectivity sequence.

We studied the pharmacology of KCNQ5 using the brain variant I (Fig. 5). Tetraethylammonium (TEA) was a poor inhibitor with an IC_{50} of about 70 mM (Fig. 5A), whereas barium was more effective (>60% inhibition at 1 mM and 0 mV; data not shown). Linopirdine and XE991, which are rather specific inhibitors of M-type currents (10, 12, 34, 35), were much more potent and inhibited KCNQ5 with an IC_{50} in the 50–70 μM range (Fig. 5A). This is higher than the values

A

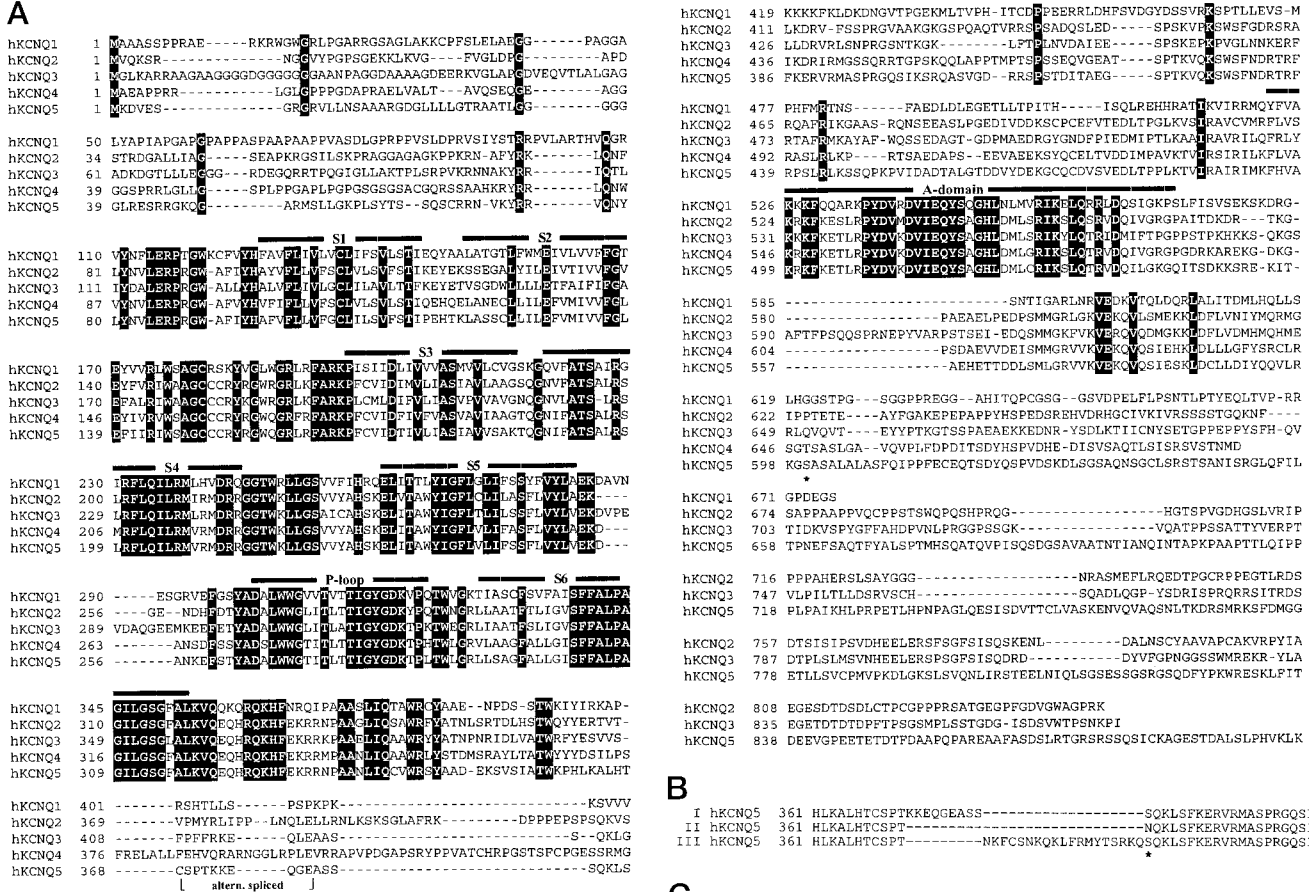


FIG. 1. Primary structure of the KCNQ5 protein. A, alignment of human KCNQ1 through KCNQ5. The brain splice variant I of KCNQ5 is shown. This includes an exon beginning at residue 373 (marked by vertical lines below the sequence). Residues that are identical in all five proteins are shown on a black background. The predicted transmembrane domains S1 through S6, the pore-forming P-loop, and the highly conserved cytoplasmic A-domain (24) are indicated by lines above the sequence. A consensus site for cAMP-dependent phosphorylation is indicated by an asterisk. B, three splice variants of KCNQ5. Variant I (also shown in A) was found by reverse transcriptase-PCR in brain, whereas variants II and III were found in skeletal muscle. Variant III introduces a second protein kinase A consensus site as indicated by the asterisk and adds six positively charged residues. C, dendrogram of KCNQ channels using the ClustalX program.

reported for KCNQ2/KCNQ3 heteromers (linopirdine, 4 μ M; XE991, 0.6 μ M) (10). When comparing these results to native M-currents, however, one should bear in mind that oocyte-expressed channels may differ in their sensitivity to inhibitors. Additionally, we identified niflumic acid as an activator of KCNQ5 currents. At 0.5 mM, it shifted the apparent P_{open} by approximately 20 mV to negative voltages (Fig. 5B). This resembles effects of niflumic acid on IsK channels (36), which are heteromers of KCNQ1 and KCNE1 (30, 31).

We also co-expressed KCNQ5 with several β -subunits of the KCNE gene family. When we expressed KCNQ5 (variant I) with KCNE1 (minK, IsK) (37) at levels that drastically activate and slow KCNQ1 currents (30, 31), we observed a reduction in the magnitude of these currents that also activated slightly slower (data not shown). The kinetic effect, however, might be explained by a superposition with a current formed by KCNE1 with xKCNQ1 which is endogenous to *Xenopus* oocytes (30). Since KCNE1 could not be detected in brain and skeletal muscle by Northern analysis (38), an interaction with KCNQ5 is

unlikely to be of physiological relevance. KCNE2 (Mirp1) (39), which shows significant expression in skeletal muscle, led to a slightly faster activation of KCNQ5 (muscle variant III). KCNE3 (39, 40), which interacts with KCNQ1 to form constitutively open channels (40), also suppressed KCNQ5 (variant I) currents in a dose-dependent manner (data not shown). The lack of drastic effects on channel properties, however, raises doubts on the physiological significance of these findings.

Inhibition of KCNQ5 by M1 Receptor Stimulation—One of the defining features of M-currents is their inhibition via muscarinic receptors. We therefore co-injected *Xenopus* oocytes with cRNAs encoding KCNQ5 and the M1 muscarinic receptor, respectively. Muscarinic stimulation led to a transient activation of Ca^{2+} -activated chloride currents that are endogenous to *Xenopus* oocytes. KCNQ5 currents were measured before muscarinic stimulation and more than 2 min after stimulating M1 receptors with either 10 μ M muscarine or oxotremorine methiodide. After this time, the Ca^{2+} -activated chloride currents had largely disappeared due to desensitization processes. KCNQ5

FIG. 2. Northern blot analysis of KCNQ5 expression. *A*, among different human tissues, expression of KCNQ5 is highest in brain and skeletal muscle. *B*, in the human brain, KCNQ5 is broadly expressed in several different regions. This includes prominent signals in the cortex, the occipital pole, frontal and temporal lobes, the putamen, and the hippocampus. *C*, the NG108-15 neuroblastoma \times glioma cell line, which has been extensively used as a model system to study M-currents, expresses both KCNQ3 and KCNQ5.

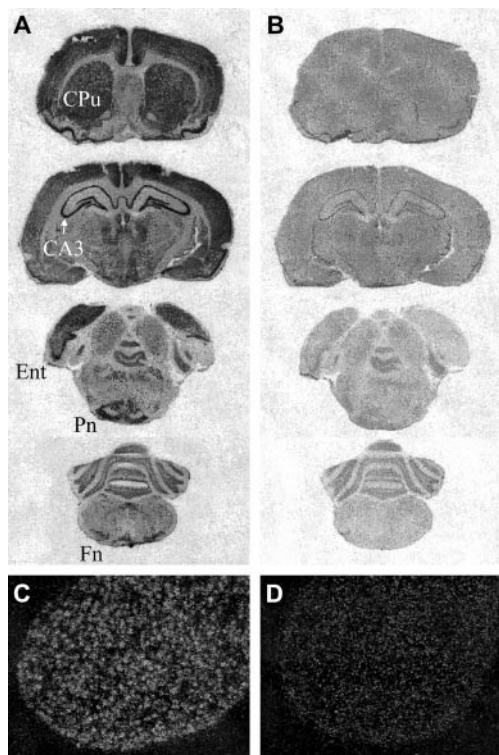
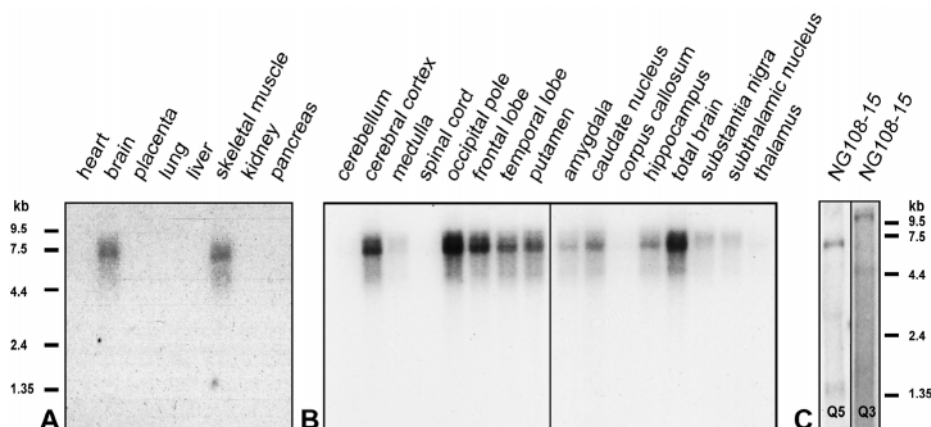


FIG. 3. *In situ* hybridization of adult rat brain sections (A) and a rat superior cervical ganglion (C). *B* and *D* are the corresponding sense controls. Consistent with the distribution determined by Northern analysis (Fig. 2*B*), KCNQ5 is highly expressed in the cortex, hippocampus, and the caudate putamen. CA3, CA3 field of the hippocampus; CPu, caudate putamen (striatum); Ent, entorhinal cortex; Pn, pontine nucleus; Fn, facial nucleus.

currents were inhibited typically by more than 80% after M1 receptor stimulation (Fig. 6). Thus, KCNQ5 also shares this type of regulation with neuronal M-currents.

Interactions with Other Neuronal KCNQ Proteins—As several KCNQ subunits can assemble to form heteromeric channels (6, 7, 9, 10), we investigated whether KCNQ5 can assemble with KCNQ2 or KCNQ3 with which it is co-expressed in many regions of the brain and in sympathetic ganglia. We co-expressed KCNQ2 with KCNQ5 using constant total amounts of cRNA but different ratios of cRNA concentrations to allow for different stoichiometries of channel assembly. In none of these co-injection experiments did the magnitude of currents significantly differ from those elicited by either homomeric KCNQ2 or KCNQ5 channels (Fig. 7*A*). Furthermore, the kinetic properties of currents could not be distinguished from a linear superposition of both currents (Fig. 7*B*). This is in contrast to

the large current increase upon co-expression of KCNQ2 with KCNQ3 (7, 9, 10). As a further test, we co-expressed KCNQ5 with a dominant negative mutant of KCNQ2 (G279S) (7) and also WT KCNQ2 with the equivalent mutant of KCNQ5 (G278S). When expressed by themselves, these mutants did not yield currents. The currents resulting from these co-expression experiments were approximately 50% of WT KCNQ5 or KCNQ2 currents (Fig. 7*A*). This current level would be expected in the absence of an interaction because 50% of WT RNA was injected to keep the total amount of cRNA constant.

Kinetic analysis revealed that currents of oocytes co-injected with KCNQ2 and KCNQ5(G278S) activated like KCNQ2 currents and that KCNQ2(G279S)/KCNQ5 injected oocytes gave currents that kinetically resembled KCNQ5 currents (Fig. 7*B*). This suggests that either these subunits do not interact or that the (presumably tetrameric) channels containing one or more mutated subunits do not yield currents. In the latter case, however, the current observed after a 1:1 co-expression of WT and mutant subunits should be reduced to less than 10% of WT if the subunits do not show any preference in assembly. Since this is not the case (Fig. 7*A*), it is concluded that KCNQ2 and KCNQ5 do not interact strongly.

Similar tests were applied to study a possible KCNQ3-KCNQ5 interaction (Fig. 7*C*). KCNQ3 by itself yields currents that are barely above background in *Xenopus* oocytes (7, 10). When co-expressed with KCNQ5, KCNQ3 increased currents (by a factor of >2) when co-injected at a low KCNQ3/KCNQ5 ratio. However, it led to a decrease in currents when present at higher ratios (Fig. 7*C*). The dominant negative KCNQ3 mutant G318S (7) significantly suppressed KCNQ5 currents. These experiments suggest that KCNQ3 and KCNQ5 form heteromers.

A still more stringent test was performed by exploiting the differential sensitivity of heteromers to inhibition by TEA. KCNQ5 is poorly inhibited by TEA (Fig. 5, *A* and *C*). This is consistent (41) with the absence of a tyrosine residue at position 283 following the highly conserved GYGDK sequence in the P-loop (Fig. 1*A*). Indeed, KCNQ2, which has a tyrosine at that position, is more sensitive to TEA, whereas KCNQ3, which lacks this tyrosine, is rather insensitive ($IC_{50} = 224$ mM) (10, 42). When KCNQ3 and KCNQ5 were co-injected, the sensitivity to TEA was decreased (Fig. 5*C*), again indicating the formation of heteromeric channels. To support this result further, we generated a mutant of KCNQ3 in which the threonine at position 323 was replaced by tyrosine (T323Y). This mutant is expected to be more sensitive to TEA. However, and probably related to the fact that even WT KCNQ3 expresses poorly in *Xenopus* oocytes (7, 10), we could not detect currents from KCNQ3(T323Y). Work on other potassium channels indicated that the affinity of the blocker TEA increases with the number of tyrosines at this position within the tetrameric channel (41).

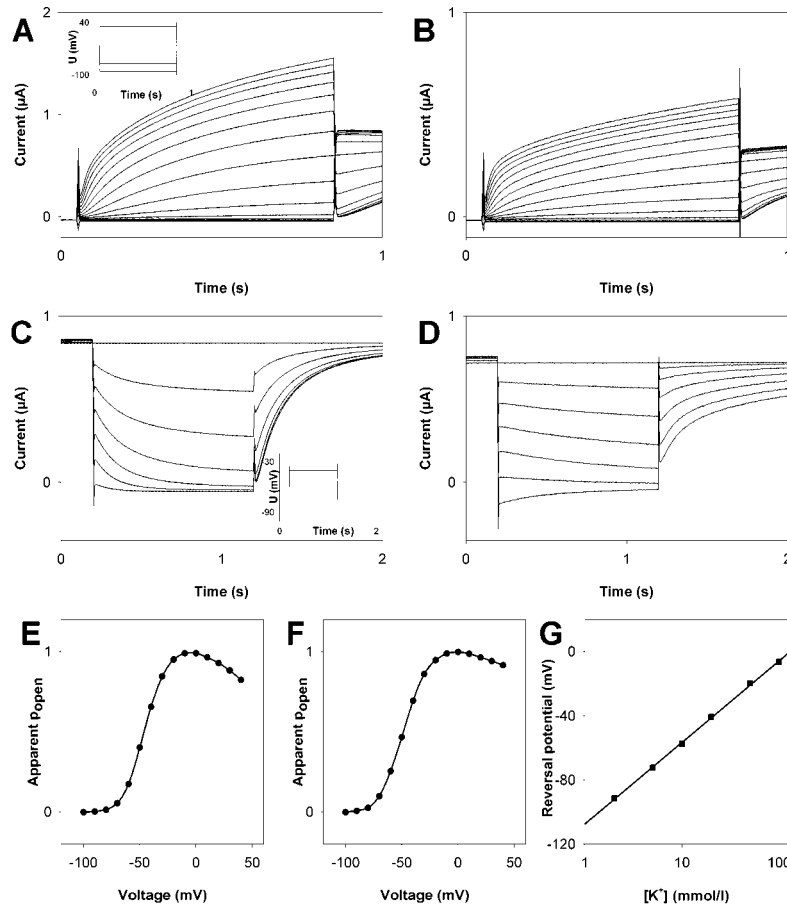


FIG. 4. Electrophysiological properties of KCNQ5. Both the splice variant I (found in brain) and splice variant III (found in muscle) were expressed in *Xenopus* oocytes and examined by two-electrode voltage clamping. Both variants activate slowly upon depolarization, but form I (A) initially activates slower than the muscle form III (B). Starting from a holding potential of -80 mV, the voltage was stepped for 0.8 s to values between -100 and $+40$ mV in steps of 10 mV, followed by a voltage step to -30 mV (see inset, A). Channel activation by depolarization was fitted (for 2 s steps) by a sum of three exponential functions. For a step to $+20$ mV, the rate constants were $t_1 = 37.2 \pm 2.2$ ms, $t_2 = 246 \pm 17$ ms, and $t_3 = 1112 \pm 91$ ms for splice variant I, whereas the constants were $t_1 = 24.5 \pm 0.8$ ms, $t_2 = 163 \pm 6$ ms, and $t_3 = 1690 \pm 46$ ms (\pm S.E., $n = 16$) for variant III. This difference in kinetics also results in different curves when a typical M-current protocol is used (C, variant I; D, variant III). Variant I induces currents that kinetically resemble M-currents. In this protocol, the membrane voltage is clamped for 1 s to voltages between -30 and -90 mV in steps of -10 mV, from a holding potential of -30 mV. This was followed by a step to -30 mV (C, inset). E and F, apparent open probabilities of variants I (E) and variant III (F) as a function of voltage obtained from tail current analysis as described under "Materials and Methods." Mean values obtained from 12 oocytes are shown. Fitting a Boltzmann equation yielded $V_{1/2} = -46 \pm 1$ mV and an apparent gating charge of $z = 2.8 \pm 0.1$ for isoform I and $V_{1/2} = -48 \pm 1$ mV and an apparent gating charge of $z = 2.5 \pm 0.1$ for isoform III. For this fit, values at potentials more positive than $+10$ mV were excluded, as these are probably affected by a second (inactivation) gating process that leads to a decrease of apparent P_{open} at more positive potentials. G, ion selectivity of KCNQ5 currents (variant I). Extracellular sodium was replaced by equimolar amounts of potassium. The reversal potential is shown as a function of the potassium concentration. This yielded a slope of 51 mV/decade potassium concentration, indicating a highly selective potassium channel. Data are from 10 oocytes from 2 different batches. E–G, the error bars are smaller than the symbols.

Thus, one would expect that KCNQ3(T323Y)/KCNQ5 heteromers are more sensitive to TEA than are the corresponding WT heteromers, and this is indeed the case (Fig. 5C). Importantly, these experiments show a change in intrinsic properties of channels by a point mutation which do not depend on the level of surface expression. Since KCNQ3 yields only very small currents in oocytes, and because KCNQ3(T323Y) does not give currents by itself, this unambiguously demonstrates the formation of KCNQ3/5 heteromeric channels.

As KCNQ5 is co-expressed with both KCNQ2 and KCNQ3 in many brain regions, we also co-expressed all three subunits at 1:1:1 cRNA ratio in oocytes. Currents could not be distinguished from a superposition of KCNQ2/KCNQ3 with KCNQ3/KCNQ5 currents (data not shown).

DISCUSSION

Our work suggests that KCNQ5, in addition to KCNQ2 and KCNQ3, contributes to M-type potassium currents in broad

regions of the brain and in sympathetic neurons. KCNQ2 and KCNQ3 co-expression yields currents that are at least 10-fold larger than those of KCNQ2 (7, 10). By contrast, KCNQ5 will lead to a more moderate increase in M-currents when co-expressed with KCNQ3 but may either increase or decrease currents when co-expressed with both KCNQ2 and KCNQ3 in the same cell. This is because the amount of KCNQ3 available to form the more "efficient" KCNQ2/KCNQ3 heteromers is reduced by binding to KCNQ5. Thus, in addition to forming a novel M-type current by itself or together with KCNQ3, KCNQ5 may also down-regulate the number of KCNQ2/KCNQ3 heteromers. Since all three KCNQ subunits are broadly, but differentially, expressed in brain, there will be various types of M-type currents in different neuron populations. Furthermore, different M-type channels may be expressed within single neurons. This will clearly be the case for NG108-15 cells, which have been used as a model system to

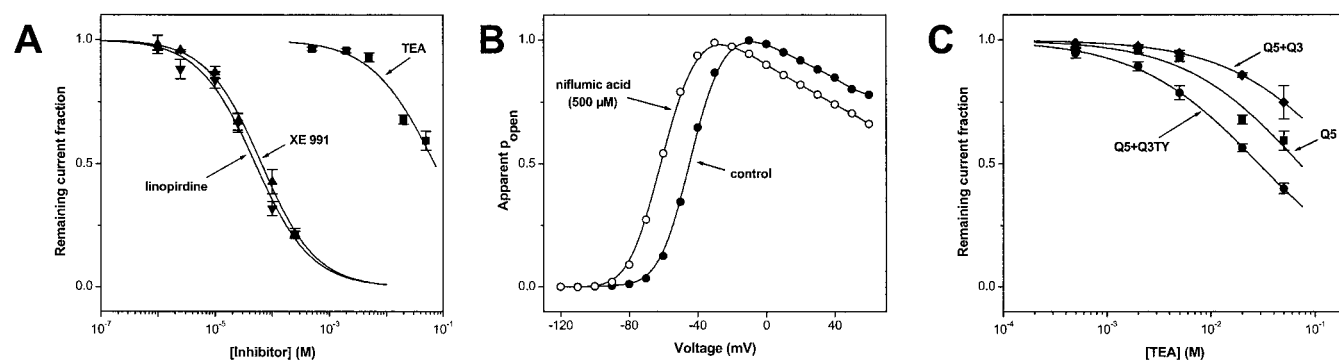


FIG. 5. **Pharmacology of KCNQ5 and KCNQ3/5 heteromers.** A, inhibition of KCNQ5 homomers by extracellular linopirdine (down triangles), XE991 (up triangles), and TEA (squares). IC_{50} values of $51 \pm 5 \mu$ M, $65 \pm 4 \mu$ M, and 71 ± 17 mM, respectively, were obtained from the plotted fit curves. B, niflumic acid alters the voltage dependence of the apparent P_{open} . In the presence of 500 μ M niflumic acid (open circles), the voltage dependence is shifted about 20 mV toward negative potentials. C, TEA sensitivity is altered in KCNQ3/5 heteromers. Co-expression of KCNQ5 and KCNQ3 (1:1) (diamonds) increased the IC_{50} value to ~ 200 mM, and co-expression with the KCNQ3 (T323Y) mutant (circles) decreased the IC_{50} to ~ 30 mM. Data points in A and C are the means \pm S.E. of 4–12 individual measurements. P_{open} was determined as in Fig. 4.

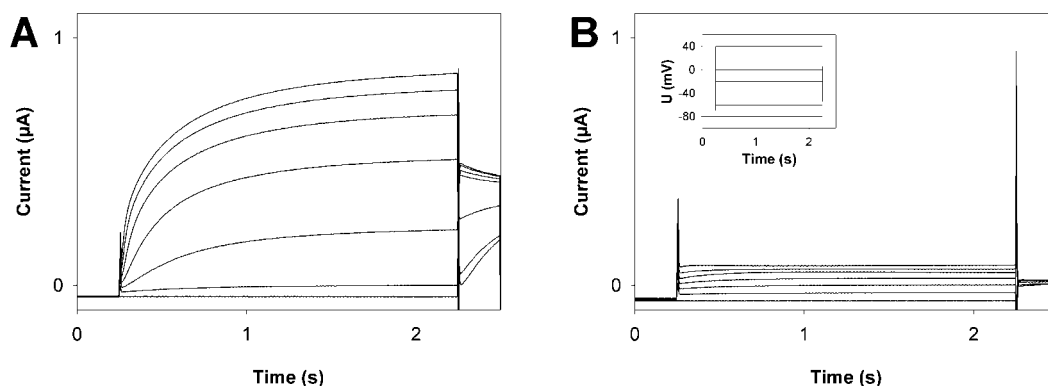


FIG. 6. **Inhibition of KCNQ5 currents by stimulating M1 receptors that were co-expressed in *Xenopus* oocytes.** A, currents before stimulating the M1 receptor; B, currents observed 3 min after applying 10 μ M muscarine. The pulse protocol is shown in the inset of B. No effect of 10 μ M muscarine or oxotremorine methiodide was found in oocytes injected with KCNQ5 alone (data not shown). Isoform III was similarly inhibited by stimulating M1 receptors (not shown).

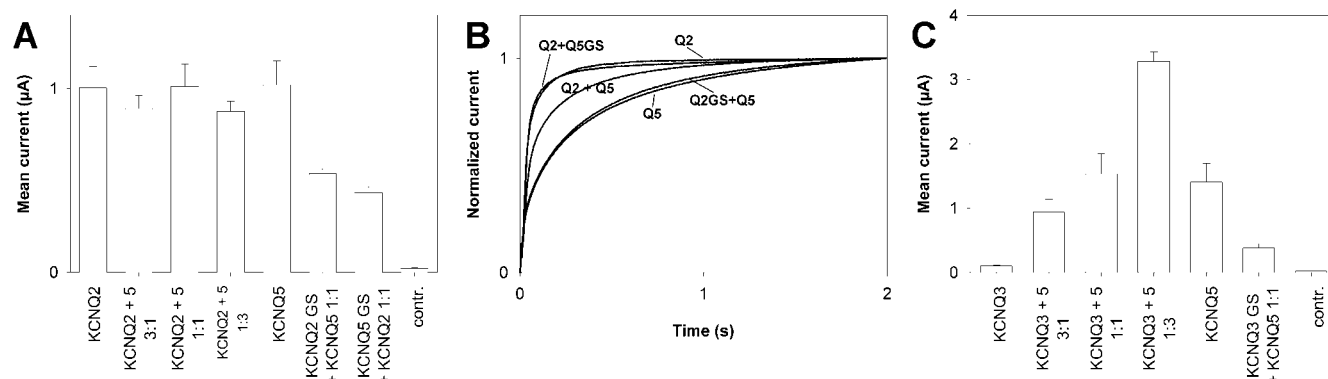


FIG. 7. **Interactions between KCNQ2 and KCNQ5 (A and B) and KCNQ3 and KCNQ5 (C).** A, currents at the end of a 2-s pulse to 0 mV from a holding potential of -80 mV of oocytes injected with different combinations of KCNQ cRNAs (always 10 ng of total amount of RNA). The current amplitude elicited by co-injecting KCNQ2 and KCNQ5 could be explained by a linear superposition of currents. Co-injection of KCNQ5 with the dominant negative mutant KCNQ2(G279S) (7) or of KCNQ2 with the equivalent mutant KCNQ5(G278S) leads to a roughly 50% reduction in current amplitude, which is consistent with a lack of interaction since only 50% of WT cRNA was injected. B, normalized current traces of experiments used for A. Currents elicited by the depolarizing pulse to 0 mV are shown. KCNQ2 (labeled Q2) activates faster than KCNQ5 (Q5), and the co-expression of both yielded currents that may be explained by a linear superposition. Co-injecting KCNQ2 with the dominant negative (and otherwise non-functional) mutant KCNQ5(G278S) yielded currents that were kinetically similar to KCNQ2, and currents from a KCNQ5/KCNQ2(G279S) co-injection resembled KCNQ5 currents. C, interactions between KCNQ3 and KCNQ5 measured as in A. KCNQ3 yields only very small currents in *Xenopus* oocytes (7, 10). Currents were enlarged when KCNQ5 was co-expressed with small amounts of KCNQ3 and were reduced when co-expressed with larger amounts. The dominant negative mutant KCNQ3(G318S) decreased currents significantly below 50% of WT KCNQ5 currents that would be expected from the injected 50% of WT KCNQ5 cRNA in this experiment.

study M-currents and which co-express KCNQ2, KCNQ3, and KCNQ5.

KCNQ5 is also prominently expressed in human skeletal

muscle (Fig. 2A). This is also true for the rat, in which Northern analysis revealed KCNQ5 expression in that tissue, but probably at lower levels (data not shown). The function of KCNQ5

in skeletal muscle is presently unclear. To the best of our knowledge, there are no reports of M-type currents in that tissue. Given the kinetic properties of the skeletal muscle splice variant III, which does not yield "M-type" gating kinetics in typical voltage clamp protocols (Fig. 4D), this may not be surprising. One report stated that linopirdine (215 μM) increased the twitch tension of mouse diaphragm muscle upon direct electrical stimulation (43). Although the mechanism is not clear, one might speculate that this is due to the inhibition of muscular KCNQ5 channels.

Mutations in either *KCNQ2* or *KCNQ3* lead to BFNC, a neonatal human epilepsy (3–5). Mutations underlying this disorder (which include *KCNQ2* gene deletions on one allele) (5) lack dominant negative effects (3, 7). The predicted loss of *KCNQ2/KCNQ3* current is small (7). The effects of mutations in *KCNQ5* on neuronal excitability are more difficult to predict and will depend on the relative expression levels of these subunits. In cells expressing only *KCNQ5*, or in cells expressing *KCNQ5* and *KCNQ3*, a loss of *KCNQ5* function would entail an increase in excitability that could lead to epilepsy. The situation is more complex in neurons expressing *KCNQ2*, -3, and -5, since *KCNQ2/KCNQ3* channels yield larger macroscopic currents than do *KCNQ3/KCNQ5* heteromers. Thus, depending on the particular situation, a loss of *KCNQ5* function could lead to either an increase or a decrease in M-current magnitude. On the other hand, certain types of *KCNQ5* mutations (e.g. dominant negative ones) could reduce overall M-type currents in neurons co-expressing all three subunits independent of their relative expression levels. Thus, *KCNQ5* may be a good candidate gene for epileptic disorders, even though no epilepsy locus has been assigned so far to human chromosome 6q14 where *KCNQ5* maps. In addition, since M-current activators may be useful for treating epilepsy, and because drugs inhibiting M-currents may be useful for treating the cognitive deficits in Alzheimer's disease (12, 34, 35), the identification of *KCNQ5* as a mediator of M-currents opens new perspectives for the treatment of neurological disorders.

Acknowledgments—We thank Susanne Fehr for help with the *in situ* hybridization of rat brain sections, Tatjana Kharkovets for the *KCNQ3*(T323Y) mutant, and Thomas Friedrich for cloning the M1 receptor cDNA. Work in this laboratory was supported by the Deutsche Forschungsgemeinschaft and the Fonds der Chemischen Industrie.

Addendum—After submission of our manuscript, Lerche et al. (44) have also reported the cloning of *KCNQ5*.

REFERENCES

- Wang, Q., Curran, M. E., Splawski, I., Burn, T. C., Millholland, J. M., VanRaay, T. J., Shen, J., Timothy, K. W., Vincent, G. M., de Jager, T., Schwartz, P. J., Toubin, J. A., Moss, A. J., Atkinson, D. L., Landes, G. M., Connors, T. D., and Keating, M. T. (1996) *Nat. Genet.* **12**, 17–23
- Neyroud, N., Tesson, F., Denjoy, I., Leïbovici, M., Donger, C., Barhanin, J., Faure, S., Gary, F., Coumel, P., Petit, C., Schwartz, K., and Guicheney, P. (1997) *Nat. Genet.* **15**, 186–189
- Biervert, C., Schroeder, B. C., Kubisch, C., Berkovic, S. F., Propping, P., Jentsch, T. J., and Steinlein, O. K. (1998) *Science* **279**, 403–406
- Charlier, C., Singh, N. A., Ryan, S. G., Lewis, T. B., Reus, B. E., Leach, R. J., and Leppert, M. (1998) *Nat. Genet.* **18**, 53–55
- Singh, N. A., Charlier, C., Stauffer, D., DuPont, B. R., Leach, R. J., Melis, R., Ronen, G. M., Bjerre, I., Quattlebaum, T., Murphy, J. V., McHarg, M. L., Gagnon, D., Rosales, T. O., Peiffer, A., Anderson, V. E., and Leppert, M. (1998) *Nat. Genet.* **18**, 25–29
- Kubisch, C., Schroeder, B. C., Friedrich, T., Lütjohann, B., El-Amraoui, A., Marlin, S., Petit, C., and Jentsch, T. J. (1999) *Cell* **96**, 437–446
- Schroeder, B. C., Kubisch, C., Stein, V., and Jentsch, T. J. (1998) *Nature* **396**, 687–690
- Tinel, N., Lauritzen, I., Chouabe, C., Lazdunski, M., and Borsotto, M. (1998) *FEBS Lett.* **438**, 171–176
- Yang, W. P., Levesque, P. C., Little, W. A., Conder, M. L., Ramakrishnan, P., Neubauer, M. G., and Blumar, M. A. (1998) *J. Biol. Chem.* **273**, 19419–19423
- Wang, H. S., Pan, Z., Shi, W., Brown, B. S., Wymore, R. S., Cohen, I. S., Dixon, J. E., and McKinnon, D. (1998) *Science* **282**, 1890–1893
- Brown, D. A., and Adams, P. R. (1980) *Nature* **283**, 673–676
- Costa, A. M., and Brown, B. S. (1997) *Neuropharmacology* **36**, 1747–1753
- Marrion, N. V. (1997) *Annu. Rev. Physiol.* **59**, 483–504
- Brown, D. A., Marrion, N. V., and Smart, T. G. (1989) *J. Physiol. (Lond.)* **413**, 469–488
- Villaruel, A. (1994) *J. Neurosci.* **14**, 7053–7066
- Stansfeld, C., Ludwig, J., Roeper, J., Weseloh, R., Brown, D., and Pongs, O. (1997) *Trends Neurosci.* **20**, 13–14
- Marrion, N. V. (1997) *Trends Neurosci.* **20**, 243–244
- Selyanko, A. A., Hadley, J. K., Wood, I. C., Abogadie, F. C., Delmas, P., Buckley, N. J., London, B., and Brown, D. A. (1999) *J. Neurosci.* **19**, 7742–7756
- Meves, H., Schwarz, J. R., and Wulfsen, I. (1999) *Br. J. Pharmacol.* **127**, 1213–1223
- Selyanko, A. A., Hadley, J. K., Wood, I. C., Abogadie, F. C., Jentsch, T. J., and Brown, D. A. (2000) *J. Physiol. (Lond.)* **522**, 349–355
- Kharkovets, T., Hardelin, J. P., Safieddine, S., Schweizer, M., El-Amraoui, A., Petit, C., and Jentsch, T. J. (2000) *Proc. Natl. Acad. Sci. U. S. A.* **97**, 4333–4338
- Lorenz, C., Pusch, M., and Jentsch, T. J. (1996) *Proc. Natl. Acad. Sci. U. S. A.* **93**, 13362–13366
- Hartmann, D., Fehr, S., Meyerhof, W., and Richter, D. (1995) *Dev. Neurosci.* **17**, 246–255
- Schwake, M., Pusch, M., Kharkovets, T., and Jentsch, T. J. (2000) *J. Biol. Chem.* **275**, 13343–13348
- Schmitt, N., Schwarz, M., Peretz, A., Abitbol, I., Attali, B., and Pongs, O. (2000) *EMBO J.* **19**, 332–340
- Nakamura, M., Watanabe, H., Kubo, Y., Yokoyama, M., Matsumoto, T., Sasai, H., and Nishi, Y. (1998) *Receptors Channels* **5**, 255–271
- Stansfeld, C. E., Marsh, S. J., Gibb, A. J., and Brown, D. A. (1993) *Neuron* **10**, 639–654
- Cloues, R., and Marrion, N. V. (1996) *Biophys. J.* **70**, 806–812
- Selyanko, A. A., and Brown, D. A. (1996) *Neuron* **16**, 151–162
- Sanguinetti, M. C., Curran, M. E., Zou, A., Shen, J., Spector, P. S., Atkinson, D. L., and Keating, M. T. (1996) *Nature* **384**, 80–83
- Barhanin, J., Lesage, F., Guillemare, E., Fink, M., Lazdunski, M., and Romey, G. (1996) *Nature* **384**, 78–80
- Pusch, M., Magrassi, R., Wollnik, B., and Conti, F. (1998) *Biophys. J.* **75**, 785–792
- Tristani-Firouzi, M., and Sanguinetti, M. C. (1998) *J. Physiol. (Lond.)* **510**, 37–45
- Lamas, J. A., Selyanko, A. A., and Brown, D. A. (1997) *Eur. J. Neurosci.* **9**, 605–616
- Zaczek, R., Chorvat, R. J., Saye, J. A., Pierdomenico, M. E., Maciag, C. M., Logue, A. R., Fisher, B. N., Rominger, D. H., and Earl, R. A. (1998) *J. Pharmacol. Exp. Ther.* **285**, 724–730
- Busch, A. E., Herzer, T., Wagner, C. A., Schmidt, F., Raber, G., Waldegger, S., and Lang, F. (1994) *Mol. Pharmacol.* **46**, 750–753
- Takumi, T., Ohkubo, H., and Nakanishi, S. (1988) *Science* **242**, 1042–1045
- Chouabe, C., Neyroud, N., Guicheney, P., Lazdunski, M., Romey, G., and Barhanin, J. (1997) *EMBO J.* **16**, 5472–5479
- Abbott, G. W., Sesti, F., Splawski, I., Buck, M. E., Lehmann, M. H., Timothy, K. W., Keating, M. T., and Goldstein, S. A. (1999) *Cell* **97**, 175–187
- Schroeder, B. C., Waldegger, S., Fehr, S., Bleich, M., Warth, R., Greger, R., and Jentsch, T. J. (2000) *Nature* **403**, 196–199
- Heginbotham, L., and MacKinnon, R. (1992) *Neuron* **8**, 483–491
- Shapiro, M. S., Roche, J. P., Kaftan, E. J., Cruzblanca, H., Macjic, K., and Hille, B. (2000) *J. Neurosci.* **20**, 1710–1721
- Tsai, M. C., Su, J. L., Chen, M. L., Fan, S. Z., and Cheng, C. Y. (1992) *Neuropharmacology* **31**, 89–94
- Lerche, C., Scherer, C. R., Seeböhm, G., Derst, C., Wei, A. D., Busch, A. E., and Steinmeyer, K. (2000) *J. Neurosci.* **20**, 22395–22400